Computer Assisted Methods in Engineering and Science, **22**: 213–227, 2015.

A CFD analysis of different human breathing models and its influence on spatial distribution of indoor air parameters

Anna Bulińska[1], Zbigniew Buliński[2]
[1] *Department of Heating, Ventilation and Dust Removal*
Silesian University of Technology
Konarskiego 22, 44-100 Gliwice, Poland
e-mail: anna.bulinska@polsl.pl
[2] *Institute of Thermal Technology*
Silesian University of Technology
Konarskiego 18, 44-100 Gliwice, Poland
e-mail: zbigniew.bulinski@polsl.pl

The computational fluid dynamics (CFD) analysis of the indoor environment in buildings requires numerical modelling of a human being (computer simulated person – CSP). There are two crucial aspects in developing reliable CSP models: the CSP geometry and the breathing model. This paper focuses on the analysis of different breathing models for application in the CFD modelling. Three breathing models were analysed: first model was restricted to constant exhalation, second model, the so-called full breathing, included constant rate inhalation, constant rate exhalation and pause period, and in the third model temporal variation of flow rate was represented by sinusoidal function. The main findings from this work show that all three models compared with experimental data gave reliable results. The spatial distribution of CO_2 concentration and velocity showed only small differences among the models in the vicinity of the mouth and above the person. It was shown that a simplified constant exhalation model can be effectively used for the CFD analysis of the indoor air quality (IAQ). However, a detailed simulation of micro-environment in the room and transport of contaminants should include complete breathing.

Keywords: breathing models, metabolic carbon dioxide, indoor air quality (IAQ), computer simulated person (CSP), CFD.

1. Introduction

Prediction of contaminant inhalation, indoor air quality and airborne infection risk requires a reliable modelling of the human interaction with surrounding. In indoor environment, occupants interact closely with their surrounding as a source of heat (thermal buoyancy flow), source of various contaminants and airflow obstacles. Airflows generated by a human being occur due to thermal buoyancy from a human body, body movements and breathing process including inhalation and exhalation of air. All this causes that any computational prediction of indoor environment state must take into account people's presence in the considered space. Rapid advancements in the computational fluid dynamics (CFD) bring nowadays interest of many researches to apply numerical modelling for prediction of indoor environment quality. However, the crucial element of the mathematical description of inhabited indoor environment is a credible mathematical model of human breathing process, which constitutes the main topic of the paper.

Experimental measurements of quantities describing conditions in the indoor environment with people are very difficult and sometimes not even possible to perform in real-life conditions with humans. Hence, in situations such as analysis of cross-infection in hospitals, air quality in trans-

portation vehicles, and prediction of contaminant distribution in indoor space and its influence on humans, experimental studies can be substituted by the CFD simulations. Recently, to simulate the breathing process, which is one of the most demanding problems in experimental studies on ventilation, breathing thermal manikins have been developed. Various applications of breathing thermal manikins in indoor environment studies can be found in [18, 21, 23, 25, 30, 31]. Similarly as in experimental studies, a key role in the reliable CFD simulation of indoor environment plays the CSP model [10–12, 22, 27]. Two main aspects of developing of the CSP models can be distinguished: the CSP geometry and mathematical description of breathing process. The subject literature shows that a simplified geometry of a human being can be effectively used for indoor air prediction. The detailed geometry is recommended when the micro-environment in the close vicinity of a human body is investigated [8, 19]. Based on these remarks, a geometrical model of the person was simplified in this study to a cuboid shape.

The second problem regarding development of the CSP model for the CFD analysis is concerned with a proper mathematical modelling of the human breathing process. The most precise sources of information about the breathing process are measurements with people. The different exhalation modes of humans may cover: breathing, talking, sneezing and coughing (the list is not exhaustive). Gupta et al. [13] experimentally studied the characteristics of exhaled airflow in breathing and talking people. Sneezing and coughing, which bring higher infectious risk, were studied in [5, 7, 14]. Usually, the results from measurements with humans are used as boundary conditions and contribute to the validation of CFD predictions. The thermo-fluid boundary conditions in CFD calculations must include exhalation flow rate, direction, species' concentration in the exhaled air, air temperature and the area of mouth or nose opening. The most commonly used parameters to characterise human breathing process are respiration frequency (RF) – the number of breaths in a minute and minute volume (MV) – the volume of expired air per minute [17]. Gupta et al. [13] distinguished the formulas for MV and RF specifically for males and females. According to this work, MV depends on body surface area, while RF depends on the weight and height of a person. Substantial information on the thermal parameters of exhaled air like temperature of exhaled air can be found in [13, 16]. Generally, people can breathe through the mouth or the nose, therefore one of the two ways of human breathing must be specified in the model as a boundary condition. Description of the breathing organ requires also the information on the area of the mouth/nose opening and the direction of the flow. The equation for the mean mouth/nose opening area and the proper angle of exhaled air distinguishing males from females was presented by Gupta et al. in [13].

Mathematical modelling of the breathing process requires functional representation of the flow rate during breathing. Experimental results with people show that human breathing can be described by the sine function for all subjects, when one breathing cycle consists of inhalation and exhalation [13], some researchers recommend also a pause period between breathing cycles [17]. Although a model of human breathing may have a significant impact on the accuracy of the numerical computations, the researchers most likely use the simplified constant exhalation models [1, 11, 15], which are easy to implement in numerical calculations and result in less time-consuming computations than full breathing model. Only a few applications of the full breathing model are presented in the literature [6, 10, 12, 22].

The objective of this paper is to study the influence of different breathing models applied in the CFD simulation on the distribution of indoor air parameters in the inhabited space. Also, the influence of different breathing models on the prediction of indoor air quality and micro-environment around human body was considered in the paper. The analysis was performed in order to answer the question whether a simplification of the breathing model affects the accuracy of the computation results.

In the present paper, three different breathing models are analysed. The sinusoidal breathing model (sine function model), and the model with constant inhalation, exhalation and pause period (for simplicity hereafter it will be called full breathing model) are compared with the breathing model simplified to constant exhalation (constant exhalation model). The accomplished work al-

lowed us to develop a recommendation for using these breathing models in the CSP depending on the simulation application.

2. Method

2.1. Outline of the method

In this study, a CFD model of air flow in the real-life room was developed. This single room is located on the third floor in a multifamily building (Fig. 1a). The room is naturally ventilated with air incoming through the micro-opening in the window and removed through the door gap. To validate the CFD model a series of experiments was carried out in the room.

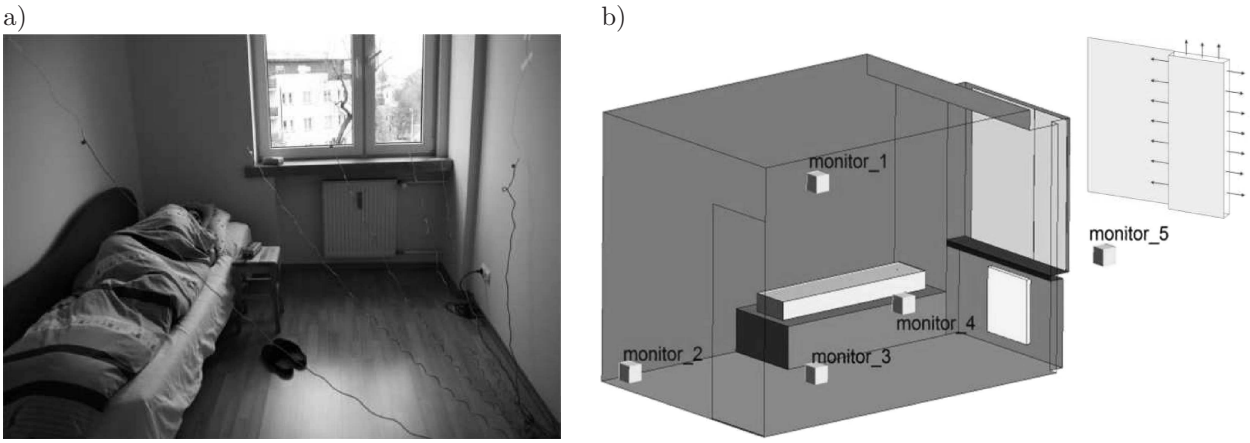

Fig. 1. a) Picture of the studied room, b) geometry of the CFD model with positions of the CO_2 monitors (monitor 1 – 20 cm under the ceiling, monitor 2 – in the room corner, monitor 3 – on the floor in the middle of the room, monitor 4 – next to bed, 45 cm above the floor).

Experiments were performed during the night in the room occupied by a sleeping person. Before the inhabitant entered the room, it was well ventilated until a uniform CO_2 concentration was reached in all monitored points. A detailed description of the performed experiments can be found in [6]. The measured quantities involved spatial distribution of the IAQ parameters (carbon dioxide concentration, temperature and relative air humidity) in the room and its surrounding. The IAQ parameters were measured using IAQ monitors PS30. Positions of the measurement points in the room were as follows: monitor 1 – 20 cm under the ceiling, monitor 2 – in the room corner, monitor 3 – on the floor in the centre of the room, monitor 4 – next to bed, 45 cm above the floor, and they are all presented in Fig. 1b. Temperature was measured at the surfaces of internal walls, window and radiator using thermocouples, while the temperature at the surface of sleeping person was measured with infrared camera. Velocity of air removed from the room was measured in the door gap by a thermoanemometer. The average value of the velocity measured in the door gap was around 0.8 m/s. Hence, the air exchange rate calculated based on the velocity in the door gap was equal to 1 h^{-1} with measurement uncertainty equal to about 13%.

Unsteady simulations of air flow inside the considered room were performed using commercial CFD software ANSYS FLUENT [2]. Initial and boundary conditions prescribed in the numerical model reflected the measured conditions inside the room during the experiment. Calculations with full breathing and sine wave model require a very small time step, because regardless of the analysed flow time, the time step size must be fitted to one breathing cycle. Moreover, in order to reproduce step change of air flow rate at mouth surface, a very short time step must be used in full breathing model when the flow direction changes (breath in changes to breath out and opposite). In the case of constant exhalation model, there is no restriction on the time step size; moreover, it can be increased with computation progress.

2.2. The CSP breathing model

As it was already mentioned, three breathing models were investigated in this work. The first model assumed constant air flow rate exhaled by a human. The second model, called the full breathing, was comprised of inhalation, exhalation and pause period. In the third model, air flow rate at mouth surface was described by sine function which fit quite well with normal human breathing process (Fig. 2). Hyldgaard [17] performed spirometer measurements of volumetric air flow rate from a breathing person. He found that a sedentary person or person performing light work exhales 6 l of air per minute with a frequency of 10 breaths per minute. According to his measurements one breathing cycle takes 6 s and consists of 2.5 s of breath in, 2.5 s of breath out, and 1 s of pause.

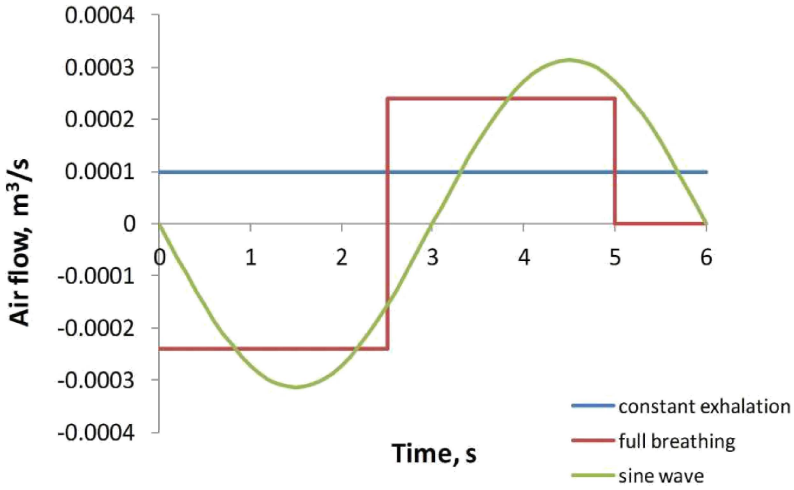

Fig. 2. Assumed models of the breathing cycle (constant exhalation, full breathing, sine wave).

The amount of exhaled air equal to 6 l per minute was assumed in constant exhalation model. The second applied breathing model was based on the results of Hyldgaard experiment [17] and it assumed that one breathing cycle consists of 2.5 s of inhalation, 2.5 s of exhalation, and 1 s of pause. The air flow rate during the inhalation and exhalation period was assumed to be constant and equal to 14.4 l/min; this value was obtained by assuming that the average value of air flow exhaled during one cycle is equal to 6 l/min.

The sine function used in the third model to describe a flow rate during breathing can be expressed as

$$\dot{Q}_b = a\sin(\beta t), \tag{1}$$

where $\dot{Q}_b$ is the instantaneous volumetric flow rate exhaled by a human, a and β are the model parameters which can be calculated using equations [13]:

$$a_x = \frac{\beta_x \cdot TV}{2}, \qquad \beta_x = \frac{\pi \cdot RF_x}{30}, \tag{2}$$

$$TV = MV\left(\frac{RF_{\text{in}} + RF_{\text{out}}}{2RF_{\text{in}} \cdot RF_{\text{out}}}\right), \tag{3}$$

where RF_x is the respiration frequency for breath in ($x = in$) or breath out ($x = out$) expressed in breaths per minute, MV refers to the volume of exhaled air per minute, TV stands for the volume exchanged in one breath. Model parameters can be computed assuming that the air flow rate breathed out by a person, averaged over one cycle, is equal to 6 l/min. Obviously, it was the same value for all the studied models. With the mentioned assumption the final expression for instantaneous air flow rate at the mouth surface can be expressed as follows:

$$\dot{Q}_b = 0.3141\sin(1.047 \cdot t). \tag{4}$$

The air exhaled by a human was modelled as a mixture of four gases: O_2, CO_2, H_2O and N_2. Generation of carbon dioxide depends on the body size and level of physical activity. Emission of CO_2 for a sleeping person was calculated from equation [3, 24]:

$$\dot{V}_{CO_2} = R_q \cdot \dot{V}_{O_2} = 3.6 \cdot \frac{0.00276 \cdot A_D \cdot M}{0.23 \cdot R_q + 0.7}, \tag{5}$$

where A_D is the body surface area in m^2, M is the metabolic activity in met (1 met = 58 W), R_q is the respiratory coefficient which has value of 0.83 for adult person taking a rest [3]. A_D value can be calculated using equation $A_D = 0.202 \cdot m^{0.425} \cdot h^{0.725}$, where m denotes weight of the person in kg and h height in m. The calculated emission of CO_2 for sleeping person was $3.4896 \cdot 10^{-6}$ m^3/h, which constitutes 3.49% (in volume) of CO_2 in exhaled air. The same values of species mass fractions in the exhaled air were assumed in all the analysed breathing models. Models with full breathing and sine wave were implemented in FLUENT as user defined functions (UDFs).

2.3. Numerical model

A three-dimensional numerical model of the room with dimensions $2.5 \times 3.9 \times 2.5$ m was built. Air infiltration to the room was modelled as an infiltration slit along the part of the window perimeter with an area of 0.0086 m^2 (Fig. 1b). The air from the room was removed by the door gap with an area of 0.008 m^2. The air change rate was calculated based on the air velocity measured in the door gap (0.8 m/s) and it was equal to 1 h^{-1}. At the infiltration slit, pressure boundary condition was assumed. Geometry of a person was simplified to a cuboid shape with dimensions $180 \times 30 \times 17$ cm^3, which suits the surface area of an adult man. Breathing through the mouth was assumed in all simulations. The rectangular mouth opening had an area of 1.3 cm^2 which is equal to values recommended in the literature for the mouth opening [10, 13, 15].

The geometry of the room was discretised with hybrid grid (Fig. 3). Structured grid was used in the main part of the room, whereas unstructured grid was employed to discretise the areas around human body, mouth opening, window and door gaps. The grid element size varied from 0.1 m for structured grid to 0.001 m for unstructured grid near the mouth. The total number of the grid elements was equal to 1 101 919. The results of the grid independence study were presented in our previous publication [6]. Numerical calculations of the flow were performed using the RNG k–ε model with enhanced wall functions, which performs best for buoyancy driven flows among all k–ε models.

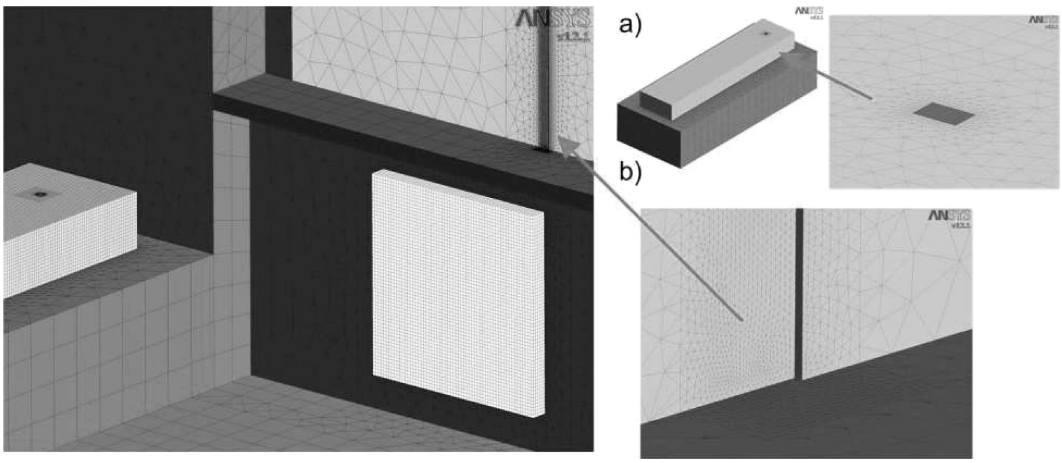

Fig. 3. Numerical grid of the computational domain: a) in the vicinity of the human subject, b) in the vicinity of the window gap.

The air was modelled as an incompressible fluid consisting of four species: oxygen (O_2), carbon dioxide (CO_2), water steam (H_2O) and nitrogen (N_2). The developed model consists of the following governing equations [9, 26, 29]:

- **Mass conservation equation** (continuity equation):

$$\frac{\partial \rho}{\partial t} + \nabla \cdot (\rho \mathbf{u}) = 0, \tag{6}$$

where ρ is the density of fluid, t is time and $\mathbf{u}$ refers to the fluid velocity vector.

- **Conservation equations for air constituents**:

$$\frac{\partial (\rho Y_i)}{\partial t} + \nabla \cdot (\rho Y_i \mathbf{u}) = -\nabla \cdot \mathbf{j}_i, \tag{7}$$

where i denotes three air constituents, namely: O_2, CO_2 and H_2O, Y_i is the mass fraction of the i-th air constituent. The mass flux of the i-th constituent may be calculated using Fick's law:

$$\mathbf{j}_i = -D_{\text{eff}} \nabla Y_i, \tag{8}$$

where D_{eff} is the effective diffusion coefficient which includes turbulence effects.

The N_2 concentration was calculated from the sum of mass fractions of all air species which should be equal to unity.

- **Momentum conservation equation**,

$$\frac{\partial (\rho \mathbf{u})}{\partial t} + \nabla \cdot (\rho \mathbf{u}\mathbf{u}) = -\nabla p + \rho \mathbf{g} + \nabla \cdot (\mu \nabla \mathbf{u}) - \nabla \cdot \tau_t, \tag{9}$$

where p is pressure, g is a vector of gravitational acceleration, μ is a molecular dynamic viscosity and τ_t is a turbulence (Reynolds) stress tensor.

- **Energy conservation equation**:

$$\frac{\partial (\rho e)}{\partial t} + \nabla \cdot (\rho e \mathbf{u}) = \nabla \cdot (k_{\text{eff}} \nabla T) - \nabla \left(\sum_i h_i \mathbf{j}_i \right), \tag{10}$$

where e is a specific internal energy, k_{eff} is an effective heat conductivity, T is fluid temperature and h_i refers to a specific enthalpy of fluid.

- **Turbulence model equations**, to close the system of governing equations one needs expression for turbulent stresses:

$$\tau_{t,ij} = -\rho \overline{u_i' u_j'} = \mu_t \left(\frac{\partial u_i}{\partial x_j} + \frac{\partial u_j}{\partial x_i} \right) - \frac{2}{3} \rho \kappa \delta_{ij}, \tag{11}$$

where μ_τ is a turbulent viscosity, κ is a turbulent kinetic energy and is δ_{ij} is Kronecker's delta.

The system of Eqs. (6)–(11) was discretised using the finite volume method. For each breathing model, the unsteady calculations were run for three hours.

Detailed numerical values prescribed at the boundary conditions in the developed numerical model are presented in Table 1.

Table 1. Initial and boundary condition assumed in the model.

Boundary conditions	Parameters
Initial air parameters in the room	T = 19°C; ϕ = 39%; C_{CO_2} = 385 ppm
Air inflow	m = 0.00812 kg/s; T = 10°C; ϕ = 60%; C_{CO_2} = 382 ppm
Air outflow	prescribed pressure equal to surrounding pressure
Air exhaled by human	T = 34°C; ϕ = 95%; C_{CO_2} = 36 000 ppm
Human body surface	T = 23.5°C covered with duvet
Room walls	T = 20°C – internal walls; T = 19°C – external wall

3. Results and discussion

Commonly, in the literature, carbon dioxide concentration is referred to as an indoor air quality indicator [4, 24, 28]. There are close relationships between carbon dioxide concentration and occupants' perception of the indoor air quality, between carbon dioxide concentration and concentration of indoor-born pollutants, and between CO_2 concentration and ventilation rates [24]. This was the argument to choose the CO_2 as a main quantity for assessment of performance of the breathing models.

Figure 4 shows comparison of the experimental CO_2 concentration curve with numerically calculated carbon dioxide concentrations for three breathing models: constant exhalation model, full breathing model and sine function model. The results are presented at four sampling points inside the room (monitor 1 – under the ceiling, monitor 2 – in the room corner, monitor 3 – in the middle of the room, monitor 4 – next to the bed). No significant differences in CO_2 concentration curves can be found in the analysed breathing models. It can be seen that all three CO_2 curves are almost identical at considered points with differences in the range of few ppm. By comparing these

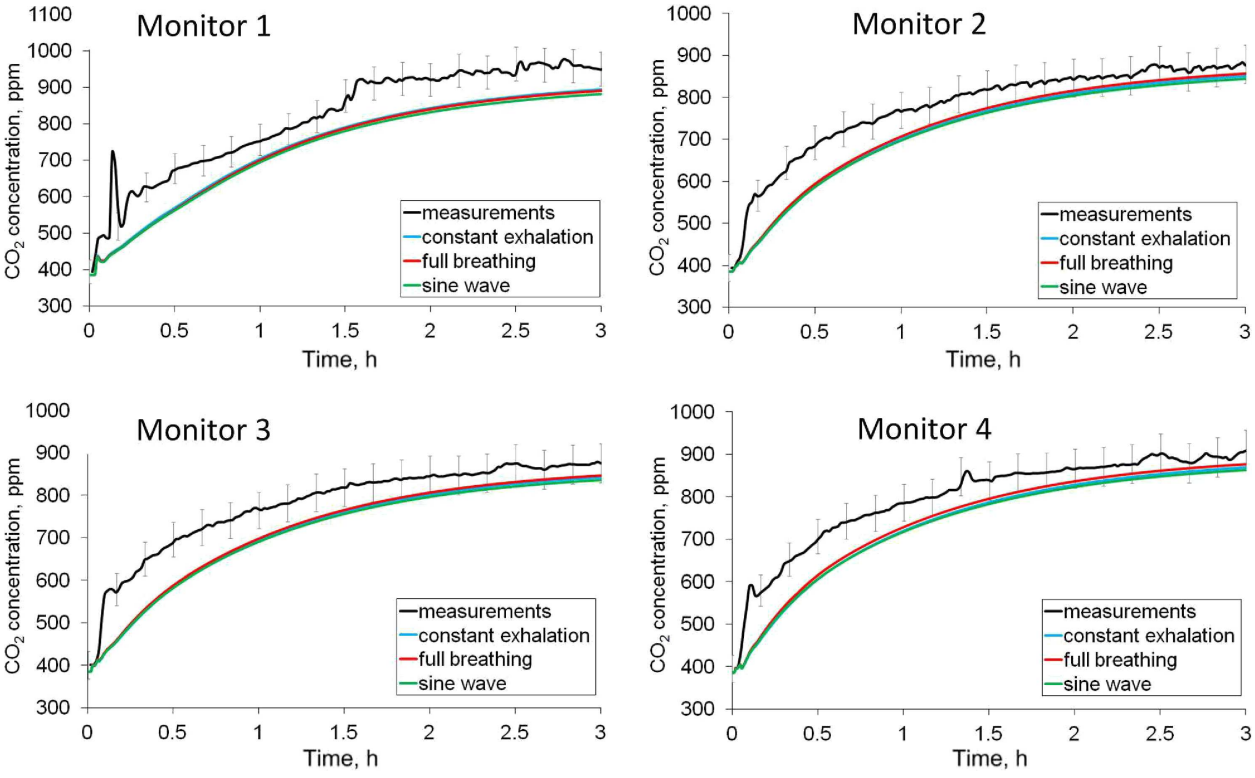

Fig. 4. Measured and numerically calculated CO_2 curves at the monitored points.

results with the experimental values of CO_2 concentration it can be seen that the calculated curves slightly underestimate the measured CO_2 concentration in the room. However, the higher differences in CO_2 concentrations are observed at the beginning of the calculations, and they gradually decrease with time. After two hours of calculations, discrepancies between the numerical results and the measurements decreased into the uncertainty range of the CO_2 sensors. The observed discrepancies between experimentally and numerically obtained CO_2 curves may be caused by few different reasons. First of all, initial conditions inside the room may not be exactly represented by the values assumed in the numerical model. Secondly, the mathematical model used to describe CO_2 emission rate from a sleeping person may not give a good estimate of this value. Finally, CO_2 emission rate from a sleeping person may change with time depending on the specific sleep stage. To preliminarily verify these hypotheses, the analysis of the influence of CO_2 mass fraction in the air exhaled by a human being on spatial distribution of carbon dioxide in the room was analysed. These analyses were carried out for constant exhalation model. Performed analyses revealed that an increase of mass fraction of CO_2 in exhaled air by 10% resulted in a better fitting of the calculated curves to the measurements (Fig. 5). In these cases, the carbon dioxide concentration increased by approximately 50 ppm at all the monitored points after 3 h of calculations, when almost steady state conditions were reached. The CO_2 emission rate from a breathing person did not change the poor fitting of computational curves to experimental ones for the initial period of calculation. It is supposed that during the measurements metabolic activity of the person going to bed was higher than after falling asleep. This suggests that in this kind of calculations the influence of changing metabolic activity of the person on calculated CO_2 emission should be taken into account.

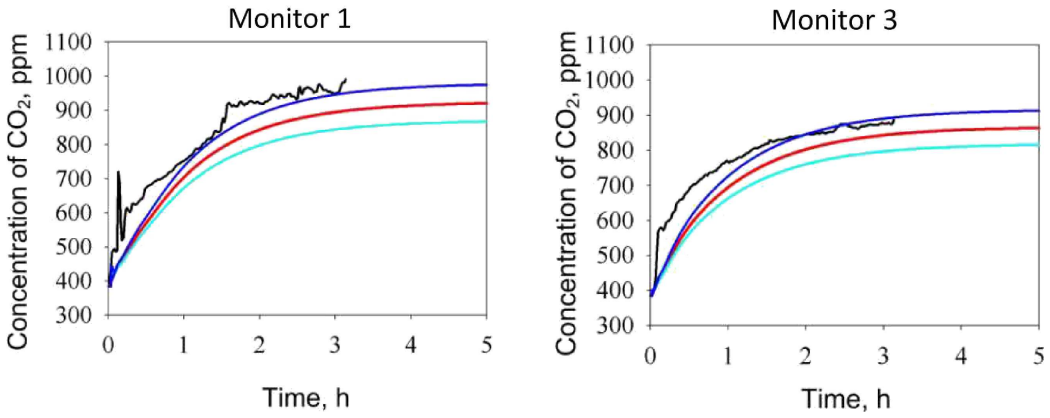

Fig. 5. Calculated CO_2 concentration curves for constant exhalation model after mass fraction changes in exhaled air for selected monitors 1 and 4.

Figure 6a presents temporal profiles of volumetric air flow rate of exhaled air for constant exhalation, full breathing model and sine wave model. The volumetric flow rates of inhaled carbon dioxide for all breathing models are shown in Fig. 6b. These values directly correspond to the concentration observed in the surrounding air. At the beginning of calculations, the average CO_2 concentration in the room was equal to 385 ppm, at the same time the CO_2 concentration in the air inhaled by a person was within the range of 500–900 ppm and after one hour the CO_2 concentration in inhaled air was in the range of 700–1200 ppm. After 2 hours of calculations the average concentration in the room increased to 830 ppm, whereas the CO_2 concentration in the inhaled air ranged between 800–1300 ppm (Fig. 7). It can be seen that a person, at the beginning of the inhalation process, breathe in air with a slightly increased CO_2 concentration in comparison to the average concentration of CO_2 in the room. The exhaled air spreads very fast and has a very limited influence on inhalation process. No significant differences in the amount of inhaled CO_2 were also found between the full breathing and sine wave model. Both models gave comparable results.

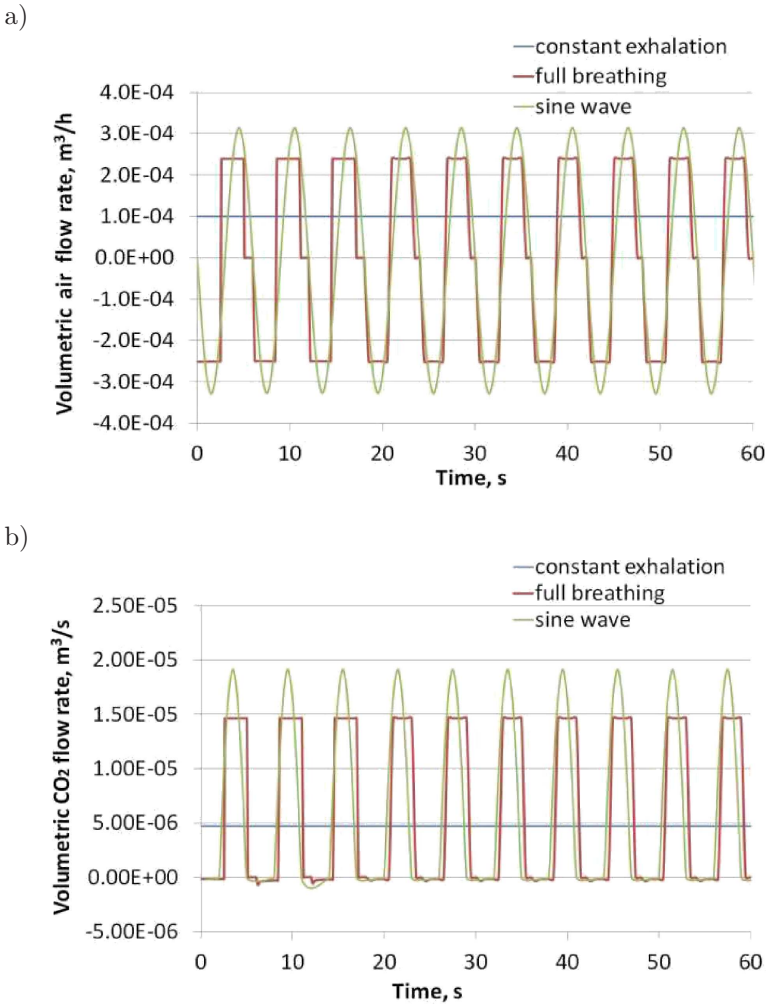

Fig. 6. Profiles of volumetric flow rate of: a) air, b) CO_2 at the mouth for the analysed breathing models.

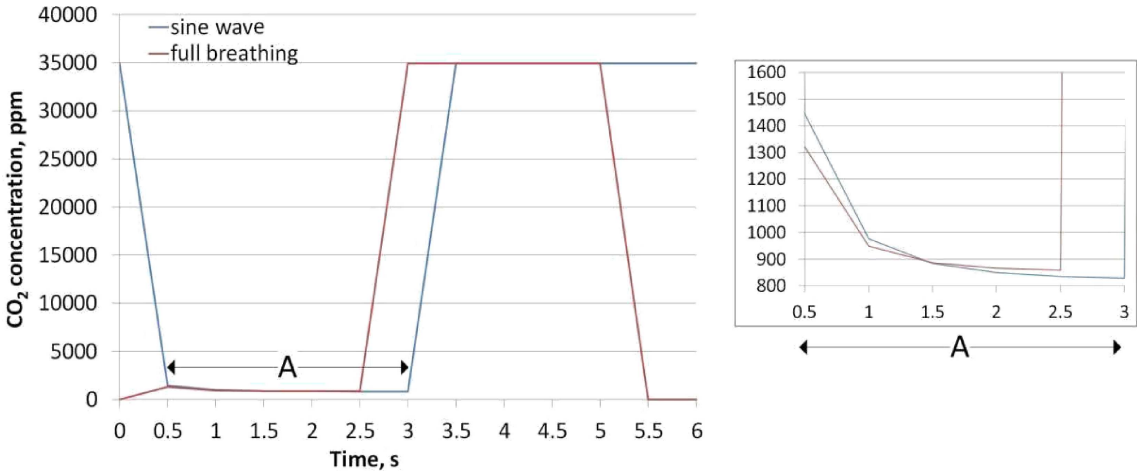

Fig. 7. Carbon dioxide concentration in inhaled and exhaled air from a mouth for one breathing cycle after 2 h of calculations, in full breathing model and sine wave model.

The obtained results allowed us to assess the indoor air quality based on the distribution of CO_2 concentration in the room. Carbon dioxide concentration contours for selected vertical and

horizontal plane for three breathing models are presented in Fig. 8. It can be seen that breathing model choice has an influence limited to the local CO_2 distribution in the room. The region with the highest discrepancies of the CO_2 concentration in the considered models was observed in the close vicinity of the person and above the person. Small differences in the spatial distribution of carbon dioxide are observed in the upper part of the room, what can be seen on the horizontal plane z = 2 m in Fig. 8. Additionally, a stratification of the CO_2 concentration was observed in the room. The higher CO_2 concentration concentrates in the upper part of the room, although, it was expected that the higher CO_2 concentration will appear at the bottom part of the room. This finding is confirmed by previous experimental studies [6, 20]. This stratification is caused by higher temperature of air breathed out by a human, since the mixing of this air with surrounding is very week under natural convection conditions, and this results in moderate stratification of CO_2 distribution and temperature. The other parameters that influence indoor air quality are the temperature and velocity of the air.

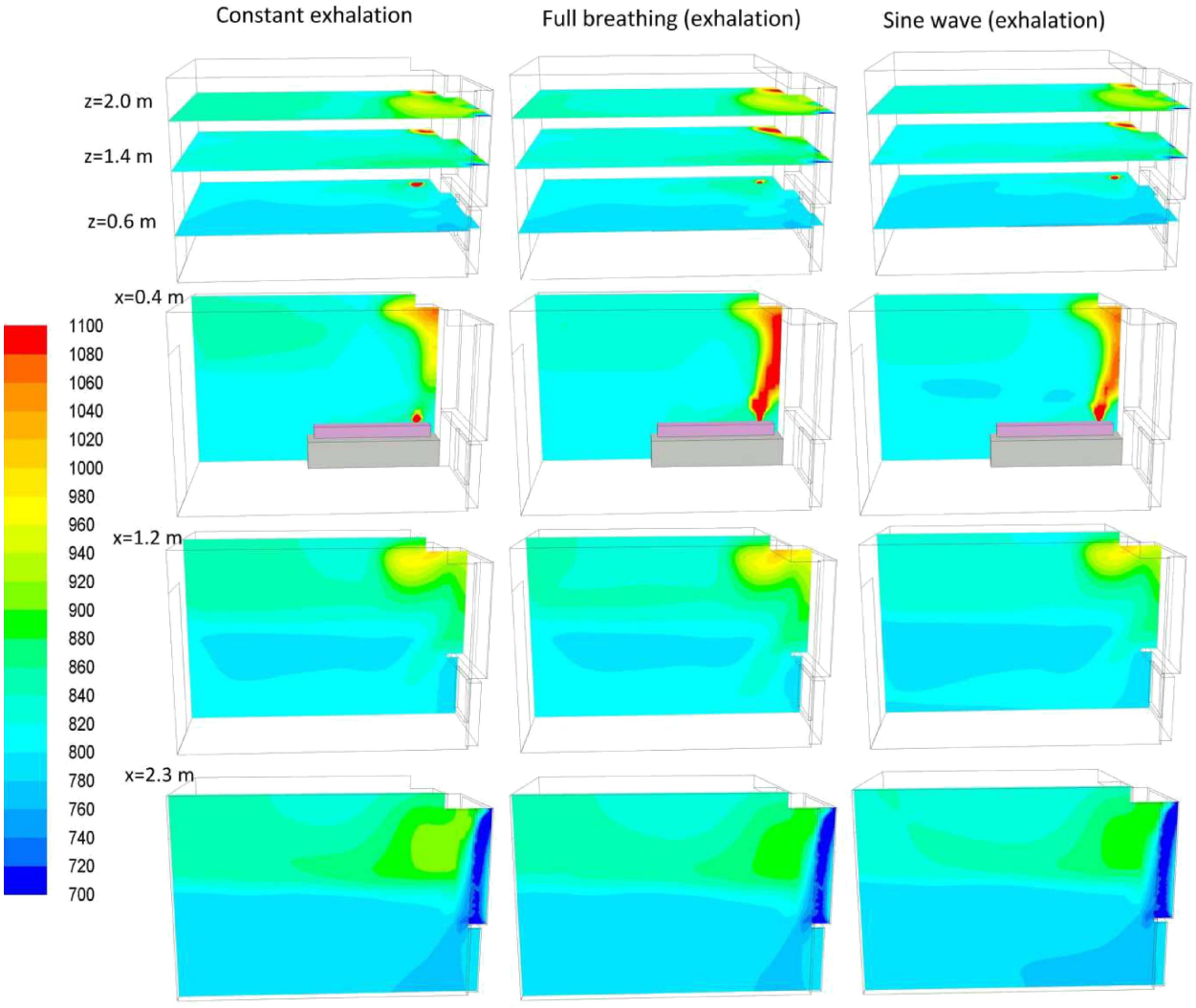

Fig. 8. Contours of the CO_2 concentration (ppm) for three breathing models at selected vertical and horizontal planes after 2 h of calculation.

A stratification of the temperature in the room was also observed after two hours of calculations and it was within the range of 18.5–20.5°C. Slight differences in the temperature profiles were observed between breathing models, but these differences are within measurement uncertainty range. In the vicinity of the sleeping person temperature profiles are very close to each other.

Full breathing model and sine function model are characterized by the higher instantaneous velocity of exhaled air equal to 1.85 m/s for full breathing and 1.2 m/s for sine wave, while in constant exhalation model the velocity reaches 0.77 m/s. However, this occurs in a very small region only a few centimetres above the mouth. Higher velocity in the full breathing model and sine function model resulted in a larger area of high CO_2 concentration above the breathing person (Fig. 8). In the model with constant exhalation, a plume with higher CO_2 concentration dilutes very fast in the region above the breathing person. Despite the velocity differences in the stream of exhaled air between the analysed breathing models, it can be noticed that this influence is limited only to region above the mouth. There is no noticeable influence on the velocity distribution in the room. The air is almost stagnant in the room, aside from the area above the person, and its local velocity does not exceed 0.1 m/s. Velocity of the air increases to 0.1–0.2 m/s in the vicinity of the sleeping person and near the window.

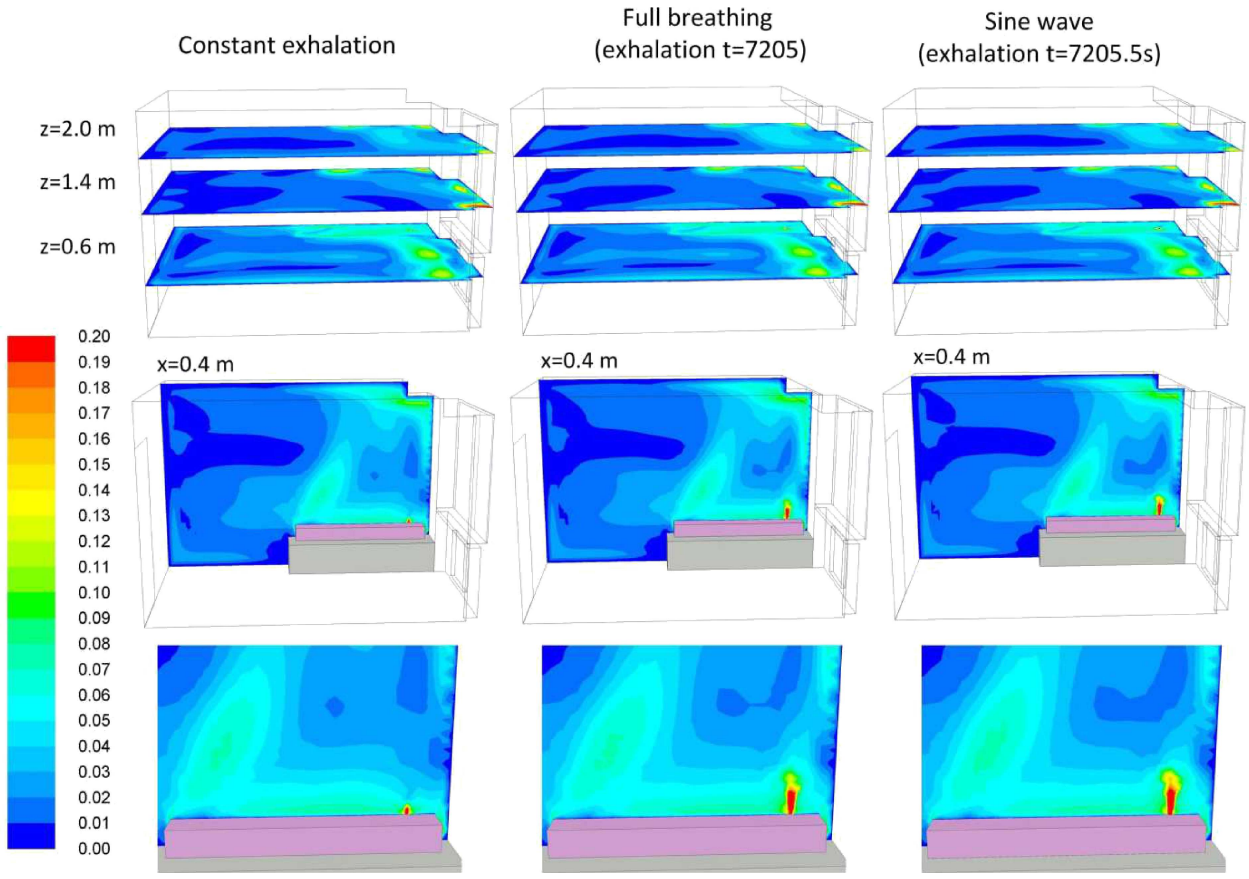

Fig. 9. Contours of air velocity (m/s) for three breathing models at selected vertical and horizontal plane after 2 h of calculation.

Application of the complete breathing model can have an influence on the predicted micro-environment around the human body. Variations of the CO_2 concentration during the breathing process for one breathing cycle, second by second, for the full breathing and sine wave models are presented in Fig. 10. Only during the first second of breathing, the air plume exhaled by human influences significantly the contaminant concentration in the vicinity of human mouth (see also Fig. 7). The CO_2 concentration in the range from 0 to 2500 ppm covers the region from the mouth entrance up to twenty centimetres above it. Further from the mouth, the CO_2 concentration in the exhaled air plume drops to the value around 1200 ppm. No significant differences in CO_2 profiles in inhaled and exhaled air were found for these two analysed models. Based on the literature information, the sine function model is the closest to the real-life breathing process among all the

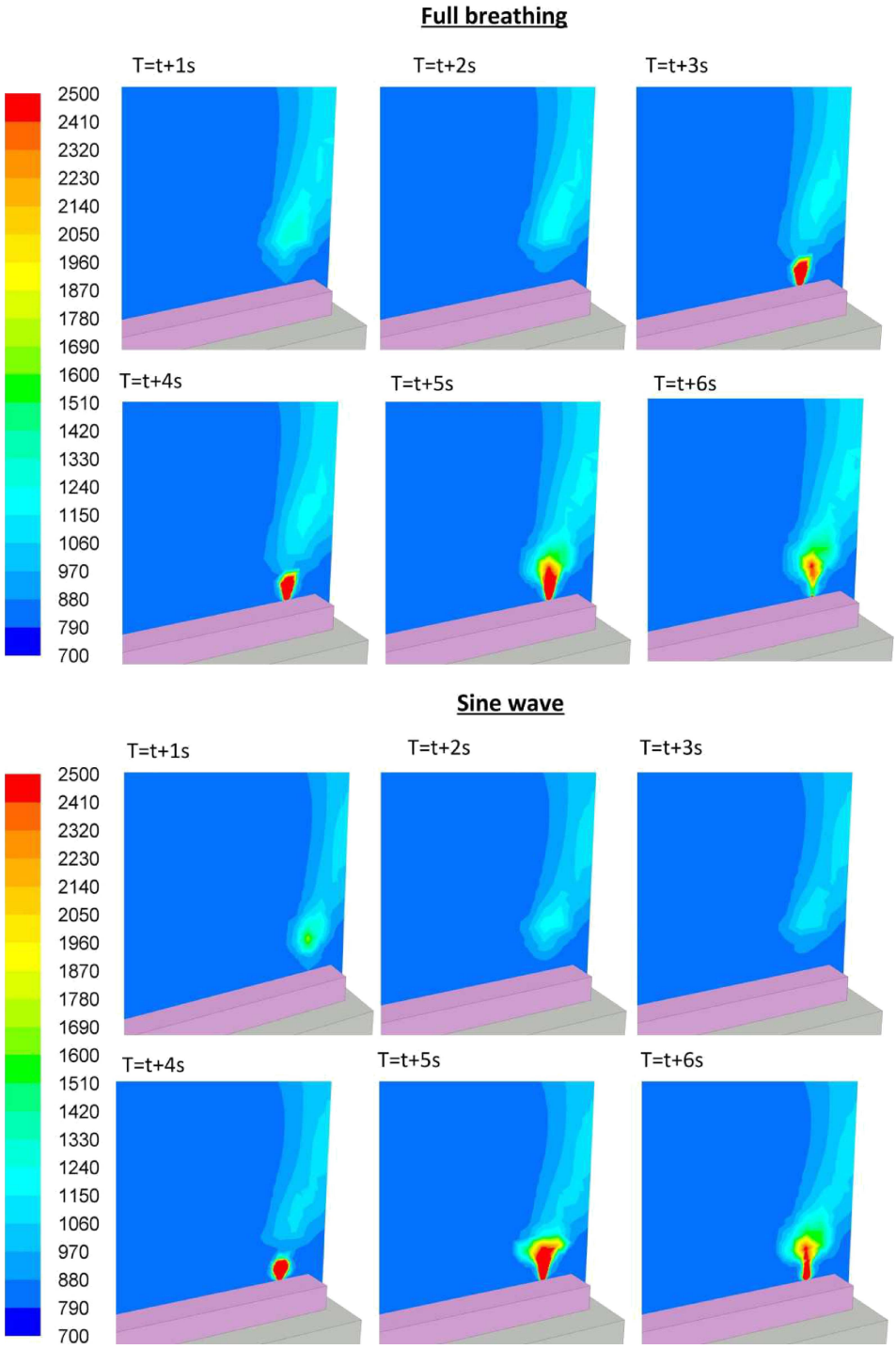

Fig. 10. Contours of carbon dioxide concentration (ppm) for one breathing cycle for full breathing and sine wave model, for time t = 7200 s.

considered models, but from the point of view of numerical calculations the differences between all three analysed models are meaningless.

The other quantities that are very useful for the analysis of spatial distribution of exhaled air parameters are path lines released from the main air inlets. The path lines of the exhaled air coloured by CO_2 concentration for analysed breathing models are presented in Fig. 11. The exhaled air with high CO_2 concentration reaches almost the ceiling of the room, then it moves towards the window, and dilutes with outdoor air and spreads around in the central part of the room. Similar

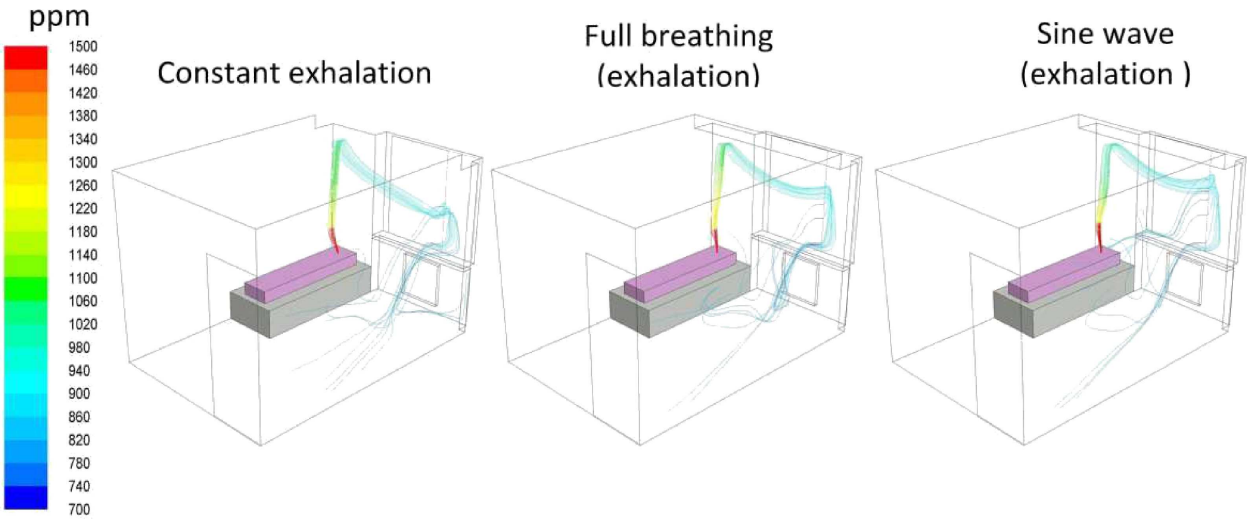

Fig. 11. Path lines coloured with carbon dioxide concentration (ppm) from the mouth surface.

path lines could be constructed for other contaminants present in exhaled air, which might be a source of cross-infections in the room. Only small differences were observed in the path lines among all the analysed breathing models. What must be taken into account in that case is that the room was well ventilated during the whole experiment (number of air exchanges equal to 1 h^{-1}). The differences in computational air flow path lines and CO_2 distribution might have been more significant in the room with poor ventilation. In the analysed case, the applied breathing models have very small influence on carbon dioxide migration in the room. The presented results of CFD calculations for three breathing models showed that each model can be successfully used to predict indoor air quality.

4. Conclusions

This paper focuses on characterisation of human breathing for CFD simulation purposes. Different breathing models can be found in the literature; however, no practical information can be found on their application range for different types of numerical studies. Based on the literature review, three breathing models were chosen to simulate breathing process in the numerical model of occupied room: constant exhalation, full breathing (with inhalation, exhalation and pause period) and sine wave model. Computation results were compared with measurements carried out in the modelled room with one sleeping person. Comparison of the different breathing models with the measurement results allowed us to assess the applicability of these models in the context of CFD modelling of indoor air quality. The analysed cases demonstrated high effectiveness of all three breathing models to model indoor air flow in the presence of a human being.

Summarising, the following main conclusions can be drawn:

- Human breathing can be effectively modelled using the CFD approach. All three breathing models gave reliable results when compared to experimental data.

- For general IAQ application, the breathing model simplified to constant exhalation is sufficient. No significant differences in the spatial distribution of the main IAQ parameters (CO_2 concentration, velocity, temperature) were observed in the room. The most important advantage of the breathing model simplified to constant exhalation is its much shorter time of calculation in comparison to complete models, and easier implementation which does not require the application of user-defined functions (UDFs).

- Analyses of the micro-environment around human body and analysis of the contaminant influence on a human being require more sophisticated breathing modelling including inhalation and exhalation of air. It seems that the sine function model should be recommended as the most similar to human breathing and giving reliable numerical results, despite that no meaningful differences between full breathing model and sine model were observed.

- In problems covering the analysis of influence of the indoor-born contaminants on human body, the full breathing cycle with inhalation and exhalation should be applied. The constant inhalation should not be used for those problems because it cannot model self-generated contaminants.

In the future study, the influence of human position (standing, seating) and ventilation rate, especially in the poorly ventilated rooms, on the distribution of indoor parameter will be analysed. Specifically, dependence between breathing models and conditions in poorly ventilated rooms will be investigated.

References

[1] I. Amezzane, A. Awada, M. Sawan, F. Bellemare. Modelling and simulation of an infant's whole body plethysmograph. *Medical & Biological Engineering & Computing*, **44**(9): 823–828, 2006.
[2] Ansys. Ansys 13.0 Product Documentation.
[3] ASTM Standard D 6245-98. Standard guide for using indoor carbon dioxide concentration to evaluate indoor air quality and ventilation. American Society for Testing and Materials. 2002.
[4] G. Beko, T. Lund, F. Nors, J. Toftum, G. Clausen. Ventilation rates in the bedrooms of 500 Danish children. *Building and Environment*, **45**(10): 2289–2295, 2010.
[5] Z.D. Bolashikov, A.K. Melikov, W. Kierat, Z. Popiolek. M. Brand. Exposure of health care workers and occupants to coughed airborne pathogens in a double-bed hospital patient room with overhead mixing ventilation. *Hvac&R Research*, **18**(4): 602–615, 2012.
[6] A. Bulińska, Z. Popiołek, Z. Buliński. Experimentally validated CFD analysis on sampling region determination of average indoor carbon dioxide concentration in occupied space. *Building and Environment*, **72**: 319–331, 2014.
[7] C. Chen, C.H. Lin, Z. Jiang, Q. Chen. Simplified models for exhaled airflow from a cough with the mouth covered. *Indoor Air*, **24**(6): 580–591, 2014.
[8] M. Deevy, N. Gobeau. *CFD modelling of benchmark test cases for flow around a computer simulated person*. HSL/2006/51: Health and Safety Laboratory, Buxton, UK, 2006.
[9] J.H. Ferziger, M. Peric. *Computational Methods for Fluid Dynamics*. Springer, 2002.
[10] N. Gao, J. Niu. Transient CFD simulation of the respiration process and inter-person exposure assessment. *Building and Environment*, **41**(9): 1214–1222, 2006.
[11] N.P. Gao, J.L. Niu. CFD study on micro-environment around human body and personalized ventilation. *Building and Environment*, **39**(7): 795–805, 2004.
[12] N.P. Gao, J.L. Niu. CFD study of the thermal environment around a human body: a review. *Indoor and Built Environment*, **14**(1): 5–16, 2005.
[13] J.K. Gupta, C.H. Lin, Q. Chen. Characterizing exhaled airflow from breathing and talking. *Indoor Air*, **20**(1): 31–39, 2010.
[14] J.K. Gupta, C.H. Lin, Q. Chen. Flow dynamics and characterization of a cough. *Indoor Air*, **19**(6): 517–525, 2009.
[15] T. Hayashi, Y. Ishizu, S. Kato, S. Murakami. CFD analysis on characteristics of contaminated indoor air ventilation and its application in the evaluation of the effects of contaminant inhalation by a human occupant. *Building and Environment*, **37**(3): 219–230, 2002.
[16] P. Hoppe. Temperatures of expired air under varying climatic conditions. *International Journal of Biometeorology*, **25**(2): 127–132, 1981.
[17] E.C. Hyldgaard. *Humans as a source of heat and air pollution*. [In:] 4th International Conference on Air Distribution in Rooms, S. Mierzwinski [Ed.]. Roomvent 1994, pp. 413–433, Kraków, Poland, 1994.
[18] X. Li, K. Inthavong, Q. Ge, J. Tu. Numerical investigation of particle transport and inhalation using standing thermal manikins. *Building and Environment*, **60**: 116–125, 2013.
[19] X. Li, Y. Yan, J. Tu. The simplification of computer simulated persons (CSPs) in CFD models of occupied indoor spaces. *Building and Environment*, **93**: 155–164, 2015.
[20] N. Mahyuddin, H. Awbi. The spatial distribution of carbon dioxide in an environmental test chamber. *Building and Environment*, **45**(9): 1993–2001, 2010.
[21] A. Melikov, J. Kaczmarczyk. Influence of geometry of thermal manikins on concentration distribution and personal exposure. *Indoor Air*, **17**(1), 50–59, 2007.

[22] S. Murakami. Analysis and design of micro-climate around the human body with respiration by CFD. *Indoor Air*, **14**: 144–156, 2004.
[23] I. Olmedo, P.V. Nielsen, M.R. de Adana, R.L. Jensen, P. Grzelecki. Distribution of exhaled contaminants and personal exposure in a room using three different air distribution strategies. *Indoor Air*, **22**(1): 64–76, 2012.
[24] A.K. Persily. *State-of-the-Art Review of CO_2 Demand Controlled Ventilation Technology and Application*. National Institute of Standards and Technology, 2001.
[25] D. Rim, A. Novoselac. Transport of particulate and gaseous pollutants in the vicinity of a human body. *Building and Environment*, **44**(9): 1840–1849, 2009.
[26] H.K. Versteeg, W. Malalaselera. *An Introduction to Computational Fluid Dynamics – the Finite Volume Method*. Longman Scientific & Technical, England, 1995.
[27] J.M. Villafruela, I. Olmedo, M. Ruiz de Adana, C. Mendez, P.V. Nielsen. CFD analysis of the human exhalation flow using different boundary conditions and ventilation strategies. *Building and Environment*, **62**: 191–200, 2013.
[28] P. Wargocki, N.A.F. Da Silva. Use of visual CO_2 feedback as a retrofit solution for improving classroom air quality. *Indoor Air*, **25**(1): 105–114, 2015.
[29] F.M. White. *Fluid Mechanics*. McGraw-Hill, 2008.
[30] C. Xu, P.V. Nielsen, G. Gong, R.L. Jensen, L. Liu. Influence of air stability and metabolic rate on exhaled flow. *Indoor Air*, **25**(2): 198–209, 2015.
[31] C. Xu, P.V. Nielsen, G. Gong, L. Liu, R.L. Jensen. Measuring the exhaled breath of a manikin and human subjects. *Indoor Air*, **25**(2): 188–197, 2015.